Second Harmonic Generation induced by poling in glasses

Evelyne Fargin, Brito Ferreira, G. Le Flem
Institut de Chimie de la Matière Condensée de Bordeaux, 87 avenue du Dr Schweitzer, 33608 Pessac cedex

Vincent Rodriguez, Thierry Buffeteau, Bernard Desbat
L. P. C. M., Université de Bordeaux I, UMR 5803 CNRS, 33405 Talence Cedex, France

The need for bit-rate capacity in telecom systems grows explosively, while fiber technology and/or integrated glass waveguides provide a means to implement very low cost devices with low insertion losses and fiber compatibility. But Glass-based devices are very limited when it comes to active functions as modulation, and it is therefore customary to employ anisotropic crystalline materials, such as lithium niobate. So the overall objective of glass makers is to increase the nonlinearity in glasses through poling. The technique consists of applying a high static field in the presence of heat and/or UV light. The aim is to induce in glass systems a non-linear coefficient sufficiently high (e.g. > 5pm/V) leading to electro-optical devices. First poling experiments had started with silica glass around ten years ago. Presently , sensible progress for understanding the poling mechanisms have been accomplished. On the other hand interesting results have been obtained for more exotic glass compositions. Nevertheless the achievement of combined nonlinear efficiencies and optic glass quality remains a challenge.

General Introduction

The merging need for growing capacity of information transport in the field of telecommunications during the ten last years is leading photons to be the ideal future information carrier. Switching and transmission times are effectively dramatically short when compared to their electronic counterparts. As new networks using glass fibers are developed across the world, new all-optical or electro-optical active systems have to be implemented to ensure functions like optical signal switching, modulation, routing, restoration…….etc. This presentation is focalized on active devices for electro-optical modulation (figure 1).

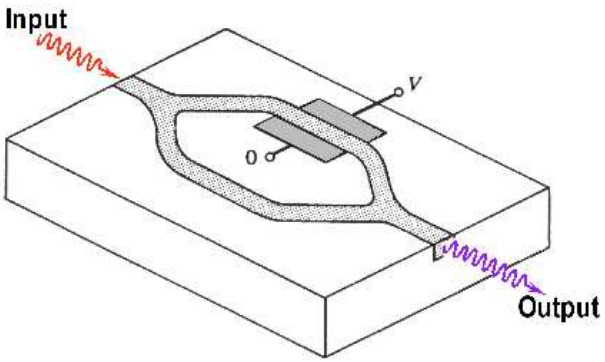

Figure 1
Schematic representation of an electro-optical modulator:
The gray zone which is submitted to a D.C. field is the nonlinear material. The output light is modulated through application of a V bias on one arm of the interferometer.

For compactness and guiding reasons, this device has to be realized in planar technology and will be in single-mode operation within the wavelengths which are used for telecommunications, today around 1.55μ.

Different materials can be considered: crystals, polymers, glasses or hybrid materials. All of them must be characterized by large second-order nonlinear optical (ONL) coefficients. Polymers have undoubtedly the best efficiencies and some components have already been commercialized (ndl.

Pacific Wave Industries Inc). The major disadvantage for these materials is their thermal instability and low irradiation damage threshold. Crystals are also interesting candidates for their large ONL coefficients and their great optical and thermal stability. Components $LiNbO_3$ based have already been commercialized (Ndl. Pirelli Society). But their elaboration cost remains prohibitive, and they are fragile from a mechanical point of view.

Inorganic glasses based devices are a possible alternative for their low cost elaboration, good thermal, optical and mechanical stabilities. Another advantage is the easier optical compatibility of such glass planar system for connection with glass fiber. As centro-symmetrical materials glass does not exhibit non zero second-order ONL coefficients. This weak point can be circumvented by subjecting the glass to the poling techniques. At the present time, whatever the technique used for poling - thermal or irradiation assisted - ONL coefficients remain lower than the values required in photonic systems.
This paper briefly summarizes the basic concepts of ONL and the first investigations of poled glasses. In a second part, the experimental procedures used for studying three types of glasses will be described. Finally the numerical data will be discussed in connection with a tentative structural characterization.

Theoretical generalities and State of the art for glasses potentialities

Basically, a polarization ($\vec{P}$) is induced in a medium by external oscillating electric fields $\vec{E}(\omega)$. This polarization can be expanded in a power series of the electric field:

$$\vec{P} = \varepsilon_0\chi^{(1)}\vec{E}(\omega) + \varepsilon_0(\chi^{(2)}\vec{E}(\omega)\vec{E}(\omega) + \chi^{(3)}\vec{E}(\omega)\vec{E}(\omega)\vec{E}(\omega)+\ldots) = \vec{P}_\lambda + \vec{P}_{n\lambda}$$

where ε_0 is the vacuum permittivity, $\chi^{(1)}$ is the linear susceptibility which accounts for the linear optical index, $\vec{P}_\lambda$ the polarization term which is proportional to the applied field and $\vec{P}_{n\lambda}$ the nonlinear polarization. $\chi^{(2)}$ and and $\chi^{(3)}$ correspond respectively to the second and third order nonlinear susceptibility tensors. For large intensities of an oscillating field $\vec{E}(\omega)$, the second term is responsible for the generation of a double frequency 2ω oscillating field called Second Harmonic Generation (SHG) and also for Pockels effect which is used in electro-optical *modulators*. However in centrosymmetric materials *which is the case of the glass*, all the components of the second-order susceptibility tensor $\chi^{(2)}$ are zero and second harmonic generation (SHG) is consequently forbidden. Nevertheless, (SHG) in bulk glasses has been induced by thermal or ultra-violet assisted poling treatment [1,4]. Basically these techniques allow the centro-symmetry to be broken. In particular, the thermal poling consists in applying a dc electric field below the *glass* transition temperature (Tg) and *in* cooling the glass before removing the dc bias. The only symmetry element which is generated during the poling treatment is an infinite order symmetry axis which is aligned along the applied z field direction. *Thus* only two coefficients in the second-order susceptibility tensor are non-zero and independent: d_{zz} and d_{zx}. The Maker-fringes analysis is the only way to characterize the low SHG signals in poled glasses [5,6]. The intensity of the transmitted generated 2ω optical signal is *recorded* for variable angles between the glass sample and the ω *incident beam*. Simulations of the fringed-shape signal allows to estimate the d_{zz} and d_{zx} values together with the generated nonlinear zone width.
The mechanism underlying the formation of the nonlinearity in bulk glass is not yet completely understood. According to Myers et al., a combination of two different mechanisms could be responsible for the induced second order nonlinear effect : a model based on charge transport of mobile ions creating a depletion region, followed by reorientation of dipoles. The permanent induced second order linearity can be expressed as the sum of both *terms* [2]:

$$\chi^{(2)} \propto \chi^{(3)}E_{dc} + (Np\beta^*/ 5kT)E_{loc}$$

The first term is related to the interaction between the residual electric field E_{dc} inside the material after removing the applied dc field and the third-order nonlinearity. The second term is the resulting macroscopic second-order nonlinearity induced by reorientations of polar bonds during the poling treatment, each of them with a permanent dipole moment p. N is the number of permanent dipole per volume *with* a microscopic hyperpolarizability β^* corrected from a local field E_{loc} which is effectively seen by each dipole.

The implementation of the field E_{dc} has been related to the migration of mobile ions (in particular Na^+) towards the cathode zone of the poled material. The result is an accumulation of sodium towards the cathode side and the creation of a few μms depth depletion zone at the anode side. Models have attributed the second order optical nonlinearity to the correlation of the third-order susceptibility and the E_{dc} field in the depletion zone [7]. The creation of a depletion zone near the anodic face with a few microns depth has been experimentally proved mainly in silica glass by LIPP (Laser Induced Pressure Probe) measurements but also in more exotic oxide glasses by XPS measurements [8-9-10]. An expended model including ion-exchange between a high mobility ion and a much lower mobility ion (related to H^+) driven by the high electric field has also been *reported* [11].

The reorientation of dipolar entities is deduced from the behavior of the poled polymers. Accordingly the ratio d_{zx}/d_{zz} value can be the signature of reorientation phenomena. Effectively, this ratio is equal to 1/3 for both migration and small dipolar moments-internal field mechanisms. However this value could be smaller than 1/3 if the coupling between the dipolar moment and the internal *field* is large enough [12].

Poling of fused silica glass has been already largely studied [1-4]. Firstly Myers et al. announced an NLO coefficient around 1 pm/V in a 5-15μm depth nonlinear under the anode during the thermal poling. Then Kazansky et al. studied the influence of pressure, poling duration, voltage and temperature parameters, the Na^+ and OH^- impurities role in the nonlinear response and succeeded to slightly improve the NLO coefficient [13-16]. They also demonstrate by the use of a Laser Induced Pressure Probe the existence of negatively charged depletion zone at the anode zone which is in accordance with the charges migration model. Qiu M. et al. tried to improve the signal by injection of anions like OH^- or F^- [17]. Whatever the composition the NLO coefficients never exceed 0.3pm/V. Finally Nazabal V. et al., as Quiquempois Y. et al. compare the behavior of herasil or infrasil (elaborated by quartz fusion) and the suprasil (elaborated by sol-gel route) varieties of silica glass under thermal poling [18,19]. Reorientations of hanging $Si\text{-}O^-$ under the anode have been evidence but cannot be proved to be involved in the nonlinearity [19]. Fujiwara T. et al. announced NLO coefficients up to 12pm/V in glassy thin films of SiO_2-GeO_2 system which have been poled under UV irradiation. They invoked the appearance of crystals, the structure of which seems to be derived from the cristobalite. Nevertheless their experimental protocol for SHG calibration, and their simulation method can be questioned.

Thermal poling of *complex* glass compositions have also been prospected. Nazabal V. et al. studied borophosphate and borate glasses and announce NLO coefficients with the same order of magnitude compared to silica glass when large *rate* of titanium or niobium oxide are introduced in the glasses compositions [20,21]. Tanaka K. et al. studied tellurite glasses and recently published a 2pm/V NLO coefficient [22]. Quiquempois Y. et al. as Liu Q. et al. used photonic versus electronic irradiation assisted thermal poling on chalcogenide glasses and obtained less than 1pm/V for the NLO coefficient [23,24].

As the different authors use various procedures for samples conditioning, poling process, SHG measurements calibration and simulation, a comparative investigation of three types of glasses was carried out; the selected glasses were the infrasil and suprasil silica commercial glasses, a tellurite glass with $70\%TeO_2$-$25\%Pb(PO_3)_2$-$5\%Sb_2O_3$ molar composition, and a borophosphate

glass with 63% $Ca(PO_3)_2$- 7% CaB_4O_7- 30% Nb_2O_5 composition. They have been studied strictly with the same experimental conditions, and ONL coefficients simulation procedure.

Experimental

1-Glass preparations and poling

Infrasil and suprasil silica 1mm thick glass samples were obtained from HERAEUS. The other samples were elaborated by the classical melting of high purity reagent powders in convenient proportions and quenching. Samples 1mm thick were cut within the same block, polished on both faces and carefully cleaned before poling.

Thermal polings were carried out in a home made apparatus working under high vacuum (10^{-8} bar). The 1mm thick glass is sandwiched between a Si wafer at the anode and a thin borosilicate plate at the cathode, then pressed on both sides by the stainless steel plate electrodes, the d.c. bias ΔV being equal to 4kV and the temperature adjusted. Once the field (4kV) is applied for 1 hour, the sample is cooled down to room temperature and the dc bias is then removed. The nonlinearity of a poled sample can be erased by an annealing treatment at 300°C without bias. The reproducibility of the poling treatment and the quality of the electric contacts were simultaneously controlled by the measurement of the poling current which is propagating through the sample.

2-Linear refractive indices and second order nonlinearity measurements

The source was a Q-switched Nd/YAG laser operating at wavelength 1064 nm. The pulse width and the repetition rate of output pulses from the laser were 200 ns and 100 Hz, respectively. The polarized source beam was split into two branches by a beam splitter. One branch recorded the fundamental intensity with a first photomultiplier; the other, which was firstly polarized, was focused on the sample with a spot of 100μm. The 2ω transmitted signal was detected by a second photomultiplier and averaged over 25 pulses. The pulse energies at the sample were no more than 200μJ for the infrared beam. The absolute calibration of the SHG intensities is obtained using a quartz z-cut taking χ_{11}=0.6pm/V for reference. This versatile experimental setup allows linear refractive index to be estimated at ω or 2ω, with a third photomultiplier, by collecting the corresponding 2-theta reflected wave around the brewster angle over the 15-80 degrees theta range. A $LiNbO_3$ crystal in phase matching condition was used as a 532 nm source to record the reflection signal. The SHG *M*aker fringes were analyzed using a new general multi-layered SHG uniaxial model including birefringence and anisotropic absorption at the fundamental and harmonic frequencies. The whole Maker fringe spectrum in pp and sp polarization configurations, where pp (resp. sp) means p-polarized (resp. s-polarized) incident pump beam and p-polarized transmitted second-harmonic beam, was recorded for the studied glass alone *and* then sandwiched between two hemicylindrical lenses (figure 2) to *increase* the complete scanning angle range inside the material. The registered Maker-fringes signal has been simulated for each configuration.

The linear refractive indices were previously determined by the Brewster angle reflection method respectively at 1064 and 532 nm allowing to estimate the dispersion (table 1).

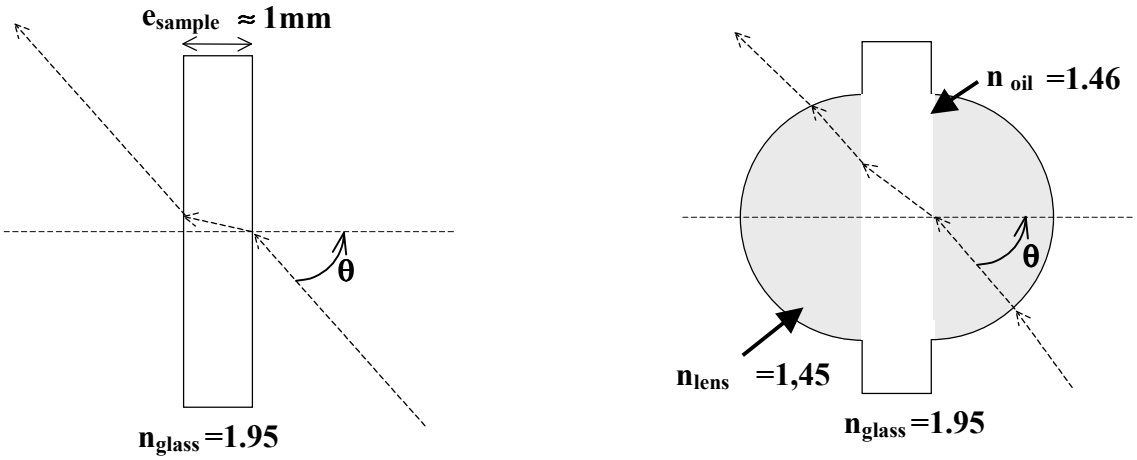

Figure 2
Using lenses allows to scan a larger probed angle range.
The optical route of the light is represented by dashed lines.

The measurements of the third order nonlinear optical susceptibilities $\chi^{(3)}$ given in table 1 were obtained using a transient absorption experiment described elsewhere [10].

3-IR Measurements

Reflectance IR spectra were recorded on a Nicolet 740 spectrophotometer equipped with a DTGS detector and a germanium-coated KBr beamsplitter. A total of 100 scans were averaged at 4cm^{-1} resolution. The spectrometer was purged with dry air to minimize atmospheric CO_2 and water vapor. Reflectance experiments were performed using an external reflection attachment (Graseby, Specac) at an angle of incidence of 12°. The optical constants (real and imaginary parts of the dielectric constant ε) have been calculated from the reflectance spectra by the Kramers-Krönig analysis. Then, the maxima of the νIm(ε) spectra give directly the frequency of the absorption bands. The both unpoled glass surfaces were analyzed before a poling treatment (figure 3a). and immediately analyzed again after control of SHG signal in the poled glass. Structural modifications after poling can be evidenced by calculating the substraction between the poled anode or cathode face reflectance signal and the corresponding unpoled face signal.

Results

1-Linear and nonlinear optical characterizations

The measured refractive indices, poling conditions, second order nonlinear coefficients d_{zz} and d_{zx} deduced from the best SHG Maker-fringes signals simulations, and measured third order susceptibilities are summerized in table 1.

At first view, the mechanism at the origin of the second-order nonlinearity is quite different between the two silica glass varieties. This observation has already been reported [18]. Usually, a pure charge migration model is supposed to explain the Infrasil silica glass behavior. Na^+ impurities migrating to the cathode during poling induce a depletion zone near the anode the depth of which is increasing within poling duration. The suprasil silica glass lower efficiency could be explained by a lower Na^+ concentration. But recently, other mechanisms, inducing larger efficiencies and involving a non-blocking anode were proposed for so high poling temperatures. While the Infrasil silica glass SHG signal simulation is unambiguous since two fringes were observed when using lenses, it is not the case for the Suprasil glass (figure 3). In this last case, only the product of ONL zone depth L and d_{zz} parameters can be strictly calculated assuming L inferior to the value which is reported in Table 1. An experimental independent

measure of the depletion zone depth is still necessary to confirm the published values by different authors.

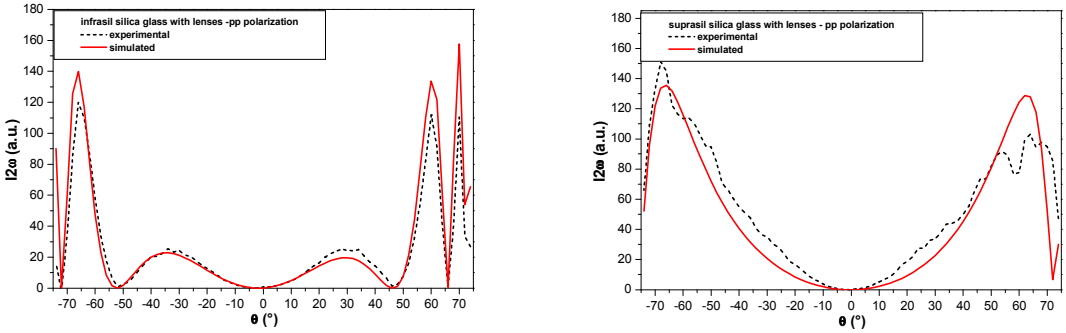

Figure 3
Maker fringes and the best simulations for infrasil and suprasil silica glasses

Both borophosphate and tellurite glasses allow to gain at least an order of magnitude for the d_{zz} parameter. For the tellurite glass, the depth of the active zone is continuously increasing with temperature. Assuming a mean field E_{dc} in the nonlinear anodic zone $\Delta V/L$ for full charge screening, the comparison with the calculated value $\chi^{(2)}/\chi^{(3)} = 2d_{zz}/\chi^{(3)}$ deduced from a pure migration model can be tempted. As far as the temperature is ≤ 225°C $\Delta V/L$ remains lower than $2d_{zz}/\chi^{(3)}$ and the result is inverted at 250°C. It can be interpreted by incomplete screening of the bias at low temperature whereas at high temperature, a contribution of the mechanism of reorientation could be postulated even if the screening is complete. But the d_{zx}/d_{zz} ratio is close to 1/3 and cannot be invoked as a proof of these reorientations.

For the borophosphate glass, a temperature evolution of both d and L parameters is not detected. Nevertheless the d_{zx}/d_{zz} ratio is different from 1/3 which is a clear indication of the contribution of the reorientation mechanism. In this case the calculated mean field $\Delta V/L$ and $2d_{zz}/\chi^{(3)}$ deduced from a pure migration model are identical.

2-Structural characterizations and mechanisms induced by the poling treament

Few structural characterizations of poled glasses have been reported. though C. Cabrillo et al. have published a neutron investigation of the bulk poled Infrasil silica glass [25]. They concluded to large microscopic alterations of the anodic poled region (about 5μm deep below the anode surface) along the direction of the poling field, involving at least next nearest Si neighbors: the shortest Si-Si distance are elongated from 3.06Å to 3.23Å in this z direction and the Si-O-Si bond angles are opened in the same direction. More recently the structural reorganizations in the Infrasil silica glass was studied by V. Nazabal et al. by XANES and IR spectroscopy . The experiments and corresponding simulations demonstrate a modification of the network and of the defects during the poling [19]. Bridging (Si-O-Si) bonds are broken and partly restored after thermal treatment. Such transformations which occur on extreme surfaces in contact with electrodes are not completely reversible. At the same time T.G. Alley et al [11] interpreted the proton conduction observed during poling, by a decrease of hydroxyl Si-OH bonds associated with an increase of non-bridging oxygen ($Si-O^-$). Simultaneously, an increase of less tensed Si-O-Si groups is observed perpendicularly to the poled surfaces which is in agreement the results given by C. Cabrillo et al, illustrating the structural anisotropic modifications produced by the poling [25].

The poled borophosphate glass studied by the RAMAN, XAFS and XPS techniques showed a progressively opening of the borophosphate network with the appearance of more non-bridging oxygen atoms on the anodic surface [10]. After an annealing treatment producing the erasure of the SHG, the bridging bonds are partly restored. IR reflectance measurements show a

slight but significant difference between poled and unpoled surfaces signals in the 960 to 1150cm^{-1} region (Figure 5).

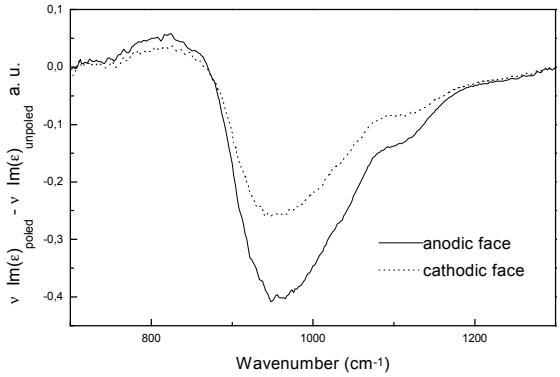

FIGURE 4.
Substraction of the IR reflectance signal of poled anode or cathode surface
from the corresponding unpoled surface signal for the niobium borophosphate glass.

The corresponding transitions are attributed to symmetrical and antisymmetrical vibration modes of terminal [PO_3^-] groups of the phosphate chains constituting the glass network. The decrease of the signal in this domain can be explained by an orientation of these groups perpendicularly to the anodic surface if the glass. On the basis of these results, the breakdown of isotropy induced by poling is evidenced. Whether such alterations can account *of* the measured SHG efficiency in niobium borophosphate glasses needs to be clarified.

Similarly, IR reflectance spectra resulting from both poled and unpoled anodic regions on the tellurite glass composition are presented in Table 1. Significant differences are observed for the phosphate bands between 800cm^{-1} and 1200cm^{-1}, i.e in region whithout tellurite bands. A decreasing of the band intensities are observed when the glass is poled, and only in the anodic region. This could be explained by a globally decreasing oscillators strength due to the remaining internal field within the anodic region, or the reorientation of all the dipolar moments during the poling treatment.

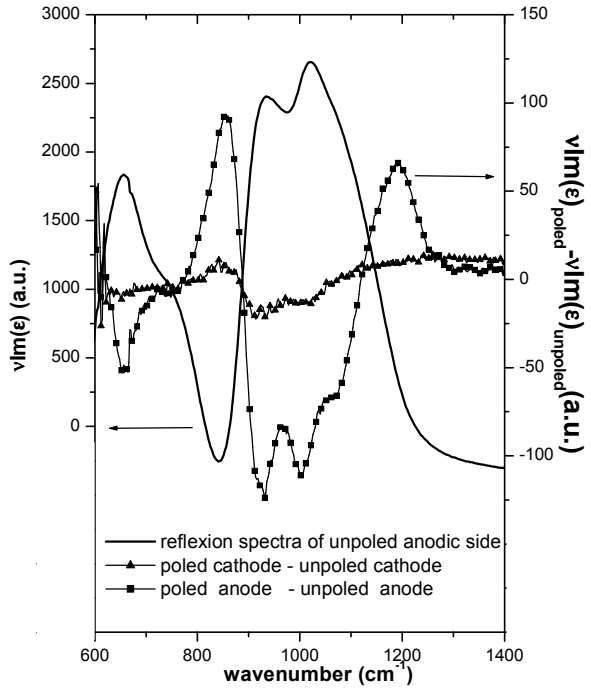

Figure 5.
Reflectance Infra-red Spectrum and differential spectra between the unpoled and then poled cathodic and anodic faces for the tellurite glass of 70%TeO_2-25%$Pb(PO_3)_2$-5%Sb_2O_3 molar composition.

Conclusion

The creation of second order non linearity by poling required strict experimental conditions for preparation of the sample and characterization of the material. The glasses were selected to explore a large range of the $\chi^{(3)}$ values. The Maker fringes technique makes possible a quantitative determination of second order NLO coefficient and/or the depth profile of the non linearity. The non linear domain is confined over a region a few micron deep at the anode side. The strength of the second order NLO coefficients of the borophosphate and of the tellurite glasses are larger than that of the two silica forms which can account for the influence of the third-order non linearity . Some contribution of reorientation effects can be deduced from the Maker fringe simulation as well as structural characterisations. Nevertheless, at the present time, poled oxide glasses are not getting the stage where they will threaten crystals such as Lithium niobate in integrated optical devices. The efficiencies rarely exceed 1pm/V. Further progress needs an investigation of new glass and probably new ceramic glass in addition to a better understanding of the fundamental mechanisms of the glass poling.

---

[1] R.A. Myers, N. Mukherjee, S.R.J. Brueck, Optics Letters, (1991), 16, 1732-1734

[2] N. Mukherjee, R.A. Myers, S.R.J. Brueck, JOSA B, (1994), 11, 665-669

[3] T. Sekiya, N. Mochida, A. Ohtsuka, M. Tonokawa, J. of Non-Cryst. Solids, 144, (1992), p128.

[4] T. Fujiwara, M. Takahashi, A.J. Ikushima, appl. Phys. Lett., 71(8), (1997), 1032.

[5] P. D. Maker et al., PHYS. Rev. Lett., 8 (1962) 21

[6] V. Rodriguez, C. Sourisseau, Non-Linear Opt., 25 (2000) 259

[7] Kazansky P. G. et al., Opt. Com., 110 (1994) 665

[8] Kazansky P. G. et al, Appl. Phys. Lett., 68 (1996) 269

[9] Pruneri V. et al., Appl. Phys. Lett., 74 (1999) 2423

[10] Nazabal V. et al., J. Of Non Cryst. Sol, 270 (2000) 223-233.

[11] T.G. Alley, S.R.J. Brueck, R. A. Myers, J. Non-Cryst. Solids, 242, (1998), 165-176

[12] Le Calvez A. et al., Eur. Phys. J., D7 (1998) 1

[13] Kazanski P. G. et al., Elec. Lett., 18 (1993) 693

[14] Kazanski P. G. et al., Elec. Lett., 30 (1994) 701

[15] Kazanski P. G. et al., Optic. Lett., 21 (1996) 468

[16] Puneri V. et al., Appl. Phys. Lett., 18 (1999) 2578

[17] Qiu M. et al., Opt. Rev., 8 (2001) 159

[18] Quiquempois Y. et al., Opt. Com., 176 (2000) 479

[19] Nazabal V. et al., J. of Appl. Phys., 88 (2000) 6245

[20] Nazabal V.et al., J. Of Solid State Chem , 133 (1997) 529-535.

[21] Nazabal V. et al., J. of Non Cryst. Sol., 290(2001)73-85

[22] Tanaka K. et al., Opt. Lett., 25 (2000) 251

[23] Quiquempois Y. et al; Elec. Lett., 36 (2000) 733

[24] Liu Q. et al., Opt. Lett., 26 (2001) 1347

[25] Cabrillo C. et al., Phys. Rev. Lett., 81 (1998) 4361

Table 1
Optical characterizations of oxides glasses

Infrasil silica glass
Refractive index $n_0 = 1.462 \pm 0.001$ ($\lambda = 532$nm)
Refractive index $n_0 = 1.450 \pm 0.001$ ($\lambda = 1064$nm)
Third Order susceptibility $\chi^{(3)} = 0.11\ 10^{-21} m^2/V^2 \pm 10\%$ ($\lambda = 800$nm)

Poling Temperature	300°C	325°C	350°C
L (μ) (±10%)	24	25	32
d_{zz} (pm/V) (±0.01)	0.05	0.04	0.03
d_{zz} L (10^{-6} pm^2/V)	1.2	1.	0.96
d_{zx}/d_{zz} (±10%)	0.32	0.31	0.30

Suprasil silica glass
Refractive index $n_0 = 1.461 \pm 0.001$ ($\lambda = 532$nm)
Refractive index $n_0 = 1.449 \pm 0.001$ ($\lambda = 1064$nm)
Third Order susceptibility $\chi^{(3)} = 0.15\ 10^{-21} m^2/V^2 \pm 10\%$ ($\lambda = 800$nm)

Poling Temperature	300°C	325°C	350°C
L (μ) (±10%)	10	14	16
d_{zz} (pm/V) (±0.01)	0.03	0.02	0.01
d_{zz} L (10^{-6} pm^2/V)	0.3	0.28	0.16
d_{zx}/d_{zz} (±10%)	0.31	0.30	0.28

Glass of molar composition $70\%TeO_2$-$25\%Pb(PO_3)_2$-$5\%Sb_2O_3$
Refractive index $n_0 = 1.986 \pm 0.001$ ($\lambda = 532$nm)
Refractive index $n_0 = 1.957 \pm 0.001$ ($\lambda = 1064$nm)
Third Order susceptibility $\chi^{(3)} = 2.44\ 10^{-21} m^2/V^2 \pm 10\%$

Poling Temperature	200°C	225°C	250°C
L (μ) (±10%)	5	7	27
d_{zz} (pm/V) (±0.01)	0.20	0.29	0.33
d_{zz} L (10^{-6} pm^2/V)	1	2.	8.9
d_{zx}/d_{zz} (±10%)	0.33	0.32	0.35

glass of 63% $Ca(PO_3)_2$- 7% CaB_4O_7- 30% Nb_2O_5 molar composition
Refractive index $n_0 = 1.801 \pm 0.001$ ($\lambda = 532$nm)
Refractive index $n_0 = 1.769 \pm 0.001$ ($\lambda = 1064$nm)
Third Order susceptibility $\chi^{(3)} = 1.08\ 10^{-21} m^2/V^2 \pm 10\%$ ($\lambda = 800$nm)

Poling Temperature	325°C	350°C	380°C
L (μ) (±10%)	8	9	8
d_{zz} (pm/V) (±0.01)	0.25	0.25	0.25
d_{zz} L (10^{-6} pm^2/V)	2.	2.25	2.0
d_{zx}/d_{zz} (±10%)	0.24	0.25	0.25